https://doi.org/10.1016/j.apenergy.2019.113832

A Statistical Modeling Approach on the Performance Prediction of Indirect Evaporative Cooling Energy Recovery Systems

Yunran Min, Yi Chen*, Hongxing Yang*

Renewable Energy Research Group (RERG), Department of Building Services Engineering, The Hong Kong Polytechnic University, Hong Kong

Abstract

Indirect evaporative cooling is well-recognized as a sustainable air-cooling solution to pursue a high quality indoor thermal environment with less energy consumption. In hot and humid areas, the application of an Indirect Evaporative Cooling Energy Recovery System (ERIEC) can cool fresh air to its dew point temperature or lower through water evaporation by using exhaust air from air-conditioned spaces. In this research, a statistical modeling approach is developed to predict the performance of the ERIEC under varying outdoor climates, taking into account possible latent heat transfer from fresh air condensation. Based on training data extracted from numerical simulation, a decision tree model was built to identify the occurrence of condensation through conditional expressions on inlet air temperature and relative humidity. A 2-level factorial design was performed to derive correlations for ERIEC performance indicators under non-condensation and condensation states, respectively. As results, the proposed practical model was validated by experimental data within the deviation of 9.52% on wet-bulb efficiency (η_{wb}) and 7.69% on enlargement coefficient (ε). A field measurement conducted in Hong Kong shows that the proposed model allows fast and precise prediction on ERIEC performance, with the measured total energy recovery of 5.85 kWh/m^2 and the predicted value of 5.40 kWh/m^2 for 30 days in cooling season. The model developed in this study can be efficiently integrated into simulation tools for the performance prediction of ERIEC assisted air-conditioning system in the building energy assessment.

Keywords: Indirect evaporative cooling, condensation, energy recovery, statistical model, performance correlation

Nomenclatures

Q	heat recovery rate, kW	A	heat transfer area, m^2
c_{pa}	the specific heat capacity of moist air, J/(kg·℃)	u	air velocity, m/s
c_{pw}	the specific heat capacity of water, J/(kg·℃)		
H	height of heat exchanger, m	Greek letters	

* Corresponding author.
E-mail address: chenyi0511@126.com (Y. Chen); hong-xing.yang@polyu.edu.hk (H. Yang)

L	length of heat exchanger, m	ω	humidity ratio of moist air, kg/kg
s	channel gap, m	η	wet-bulb effectiveness
n	number of channels	ε	enlargement coefficient
R_{con}	condensation ratio	σ	surface wettability
m	air mass flow rate, kg/s	ρ	density, kg/m^3
h	heat transfer coefficient, W/m^2·℃		
h_s	heat transfer coefficient between secondary air and plate surface, W/m^2·℃	Subscripts	
h_m	mass transfer coefficient, kg/m^2·s	c	condensation
h_{fg}	latent heat of vaporization of water, J/kg	e	evaporation
$E_{recovery}$	energy recovery, kWh	s	secondary air
i	enthalpy of moist air, J/kg	p	primary air
RH	relative humidity of moist air	w	water film
ω_{t_w}	the moisture content of saturated air at plate surface temperature, kg/kg	dew	dew point temperature
Q_{sen}	sensible heat, W	cw	condensate water film
Q_{lat}	latent heat, W	ew	evaporation water film
A_{ratio}	ratio of heat transfer area to primary air flow volume, m^2/(m^3/s)	wb	wet-bulb temperature
NTU	number of heat transfer unit	sat	saturated humidity
m_{ratio}	ratio of primary to secondary air flow volume	in	inlet of air channel
V	air flow volume, m^3/s	out	outlet of air channel

1. Introduction

As the increasingly serious circumstance of energy shortage and environmental pollution worldwide, many efforts have been made to develop sustainable air cooling technologies with low carbon emission and considerable energy efficiency [1]. Indirect Evaporative Cooling is an attractive alternative air-cooling solution due to its simple operation, low cost and non-CFC usage [2], [3]. In an indirect evaporative cooler (IEC), the heat of primary air is absorbed by water evaporation process and taken away by the secondary air in wet channels, so the primary air in dry channels can be cooled without any moisture added. The IEC has developed rapidly over the few decades with many effects made on heat and mass transfer modeling,

configuration optimization, novel heat exchangers design, hybrid systems development and energy performance evaluation [4], [5].

The basic types of IEC are applicable for sensible cooling-dominant buildings in a dry climate [6], [7], with a large number of installations found in hot and arid (or moderate humidity) regions. Bajwa et.al [7] investigated the comfort enhancement potential of evaporative cooling in a tested domestic building in the hot-arid maritime desert climate of Saudi Arabia. Maheshwari et.al [8] compared the operation performance of a commercial plate-type IEC in coastal and interior locations of Kuwait, where the seasonal energy saving differs a lot. Delfani et.al [9] tested an experimental set up of combined IEC+PUA system and evaluated its energy reduction capability in Iran by an analytical method. However, it is uncommon to find data reported the tested performance of IEC applications in hot and humid regions, as the conventional IEC is restricted by the insufficient cooling capacity under wet climates [10]. Recent studies show that an indirect evaporative cooling energy recovery system (ERIEC), which combines the indirect evaporative cooling and mechanical air-conditioning system [12], [13], can break the regional limitation of IEC and extend its application in humid areas. With the IEC employed as a pre-cooling unit for air conditioning system, the ERIEC system can recover energy from room exhaust air, possessing promising energy-saving potential and application prospects in hot and humid subtropical regions [14].

Developing mathematical models on IEC has been one of the research focuses to facilitate the further energy-saving potential investigation. As numerical models become more mainstream in solving complicated configuration and simultaneous heat and mass transfer process, a number of numerical approaches have been used to derive the IEC models with experimental validation. The widely used numerical models are mainly based on finite difference method [15], [16], [17], [18], [19], Newton iteration method based on EES (Engineering Equation Solver) [20], [21], [22], finite element method based on COMSOL Multiphysics software [10], [23], [24], Runge-Kutta method [25], [26], and finite volume method based on computational fluid dynamics (CFD) simulation platform [27], [28], [29], [30]. Among the above-mentioned models, the majority of works only considered the sensible cooling of primary air, which is suitable for dry and moderate climate areas. However, when an IEC is used as an ERIEC system which recovers energy from exhaust air in the wet climate areas, the fresh air can be cooled below its dew point temperature with dehumidifying effect. Several researchers have studied the numerical models of ERIEC system with experimental validation [17], [31], [32], [33], [34], taking into account the condensation deriving from highly humid fresh air. Chen et al. [31] firstly proposed a numerical model for counter flow IEC in the presence of condensation from primary air. The reduction of the primary air humidity and the latent heat transfer rate was validated by experiments with the discrepancy of 7.9%. Min et al. [17]

established a 2-D numerical model for cross-flow IEC and compared the performance of cross-flow and counter-flow IEC under condensation states. The optimal design parameters and operating parameters of IECs were proposed for both counter and cross-flow configurations. Pandelidis et al. [34] studied the condensation process that occurs in the product air channels of the IEC. The effect of the influential factors was identified for different IEC exchanger configuration. Meng et al. [33] conducted the visualized experiments on cross-flow IEC with a transparent cover plate. The turning point for the operation condition changed from non-condensation to partial and total condensation was investigated.

Besides the numerical models, some practical models have been developed and fitted into building energy simulations with improved calculation speed as well as satisfying accuracy in engineering application [35], [36], [37], [38]. To derive the practical predictive models, the combined effects of various parameters were determined by using statistical methods based on data extracted from experiment or numerical models. Kim et al. [35] used a multiple linear regression method to derive a function containing major design parameters to predict the thermal performance of IEC. The data for statistical analysis were generated by the ε-NTU method. The predicted values agreed well with the experimental data. Cui et al. [36] fitted the simulated results as functions of each dimensionless group for counter-flow RIEC. The model was validated by experimental data within a discrepancy of 12%. Pandelidis and Anisimov [37] presented a simplified model to identify the influential factors of M-cycle IEC by utilizing response surface methodology. The model was validated by comparing the predicted response with the experimental data. In addition, some soft computing statistical tools were also applied to analyze the performance of IEC, including artificial neural networks (ANN) [39], group method of data handling (GMDH) [40], [41] and genetic algorithm (GP) [42]. Jafarian et al. [40] developed a precise model for a dew-point IEC by using GMDH-type neural network with training data extracted from a numerical model. The model can be employed with a quick calculation process to optimize the design parameters of the IEC based on climate data. Sohani et al. [39] used five different models to describe the performance of the desiccant enhanced evaporative air conditioning system. The stepwise regression approach was found to be the best model with the least error compared to experimental data.

The ERIEC can significantly reduce the energy consumption for air-conditioning by handling both the sensible and latent cooling loads of the fresh air, possessing great application potential in hot and humid regions. It was observed from previous works that the existing research on the model development of ERIEC only focused on numerical approaches which require long computational time due to the iterative process. The simplified predictive models derived by statistical methods can combine the mutual influences of various parameters, and be easily integrated into simulation tools for building energy assessment.

However, few attempts have been made to develop the practical predictive models on both sensible cooling and dehumidifying performance for the total energy recovery evaluation of the ERIEC system. To better investigate the energy saving potential of ERIEC in hot and humid regions, a practical model is required to efficiently predict the energy recovery performance in the presence of possible condensation from fresh air under the ever-changing operating conditions.

Based on the research gap identified from existing literature, this paper focused on a statistical modeling approach in practical use to evaluate the performance of ERIEC applied in hot and humid regions. Firstly, by extracting the training data from an established numerical model under a wide range of simulation cases, a decision tree model was built for the classification on ERIEC operation conditions with or without condensation. Secondly, a 2-level factorial design was performed based on the selected parameters to correlate the performance correlations for non-condensation and condensation states respectively. For validating the proposed model, the model-predicted results were compared with experimental data on both sensible and latent heat recovery efficiency. Moreover, a 30-day field-measurement was conducted in a trial system in Hong Kong to estimate the model-predicted energy recovery performance of ERIEC under varying outdoor climate. The developed practical predictive model can help to promote the wider application of ERIEC in target regions by providing an efficient prediction for building energy assessment.

2. Numerical simulation

The numerical model of IEC, which serves as the foundation to drive the practical predictive model of the ERIEC system, is briefly presented in this section. In the ERIEC system, as shown in Fig. 1, an IEC is installed before an air-handling unit to pre-cool the fresh air (primary air) by fully making use of the cool and dry exhaust air (secondary air) from air-conditioned spaces in a building. Large wet-bulb depression of the secondary air can be achieved by using the exhaust air to evaporate the water in the wet channels, which facilitates the primary air cooling process in the dry channels. Plate type IECs are commonly manufactured and widely used in the current markets. It has great potential to be adopted in an ERIEC system to provide both sensible cooling and dehumidifying for buildings in the hot and humid areas. In this study, the plate type cross flow IEC is considered as the main component of the studied ERIEC system.

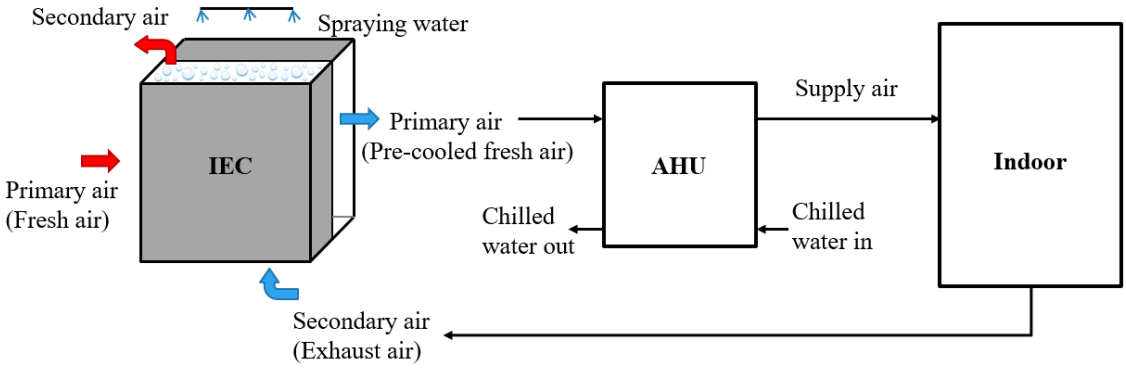

Fig.1. System diagram of ERIEC

2.1 Model description

The numerical model of IEC can provide precise solutions for the coupled heat and mass transfer process. In humid regions, the possible condensation on the primary air side of IEC should be taken into consideration. Based on the ε-NTU method [43], the governing equations for energy conservation and mass balance in 2-dimensional cross flow IEC model are as follows. The differential element in the numerical model of cross-flow IEC is presented in Fig. 2. The details of assumptions and simplification made in the model are presented in Ref. [17].

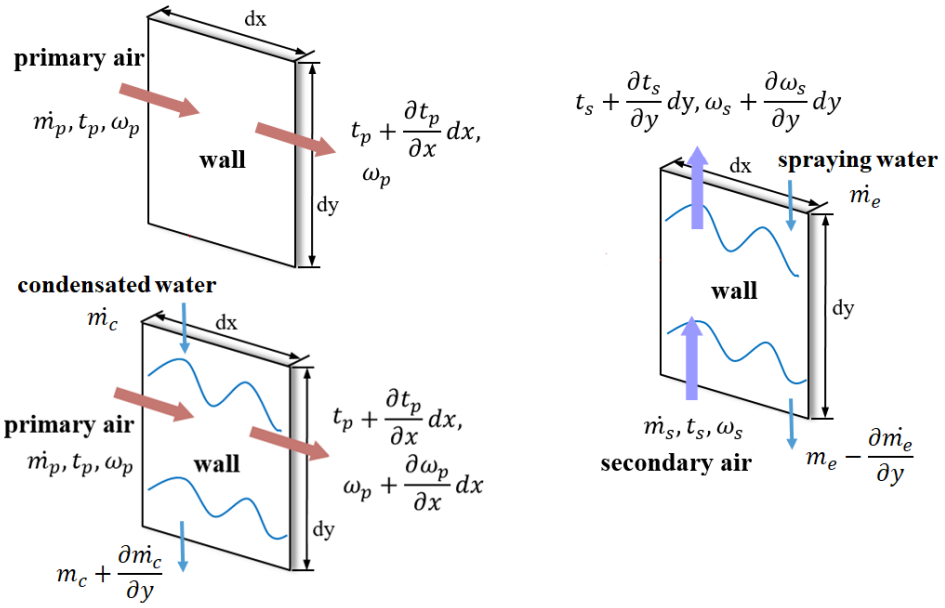

(a) primary air side (with and without condensation) (b) secondary air side

Fig. 2 Schematic view of the differential element in cross-flow IEC model

For energy balance of the secondary air:

$$h_s(t_w - t_s) \cdot dxdy + h_{fg}h_{ms}(\omega_{t_w} - \omega_s)\sigma \cdot dxdy = \dot{m}_s \frac{\partial i_s}{\partial y} \cdot dy \quad (1)$$

For mass balance of the secondary air:

$$h_{ms}(\omega_{t_w} - \omega_s)\sigma \cdot dxdy = \dot{m}_s \frac{\partial \omega_s}{\partial y} \cdot dy = \frac{\partial m_e}{\partial y} \cdot dy \quad (2)$$

For energy balance of the evaporation water film:

$$\dot{m}_s \frac{\partial i_s}{\partial y} - c_{pa}\dot{m}_p \frac{\partial t_p}{\partial x} = c_{pw}t_{ew}\frac{\partial m_e}{\partial y} \quad (3)$$

For energy balance of the primary air (without condensation):

$$h_p(t_p - t_w) \cdot dxdy = c_{pa}\dot{m}_p \frac{\partial t_p}{\partial x} \cdot dx \quad (4)$$

When the plate surface temperature is lower than the dew point temperature of primary air, i.e., $t_{dew,p} > t_w$, the condensation could take place and a new set of governing equations should be established. Therefore, Eqs. (3) - (4) can be replaced by:

$$h_{mp}(\omega_{t_w} - \omega_p) \cdot dxdy = \dot{m}_p \frac{\partial \omega_p}{\partial x} \cdot dx = -\frac{\partial m_c}{\partial y} \quad (5)$$

$$\dot{m}_s \frac{\partial i_s}{\partial y} - \dot{m}_p \frac{\partial i_p}{\partial x} = c_{pw}t_{ew}\frac{\partial m_e}{\partial y} + c_{pw}t_{cw}\frac{\partial m_c}{\partial y} \quad (6)$$

The inlet boundary conditions of both primary air and secondary air channels are defined by:

x = 0: $t_p = t_{p,in}$, $\omega_p = \omega_{p,in}$, $m_c = 0$.

y = 0: $t_s = t_{s,in}$, $\omega_s = \omega_{s,in}$.

y = 1: $m_e = m_{e,in}$.

Where, x=0 are the inlet of primary air; y=0 and y=1 are the bottom and top of the heat exchanger.

To solve the numerical models of IEC in counter- and cross-flow configurations in the presence of condensation, the finite difference method was employed and the detailed iteration process was presented in previous studies [17], [31]. The established numerical model has been validated by the experiments under operation conditions with or without condensation [32]. Good agreement can be found between the simulation and experimental results with the discrepancies of 5.9% for $t_{p,out}$ and 2.4% for $\omega_{p,out}$.

2.2 Performance indexes

Wet-bulb effectiveness (η_{wb}) and enlargement coefficient (ε) can be used to evaluate the performance on sensible and latent heat recovery of ERIEC respectively, they are expressed as:

$$\eta_{wb} = \frac{t_{p,in} - t_{p,out}}{t_{p,in} - t_{wb,s}} \quad (7)$$

$$\varepsilon = \frac{Q_{sen} + Q_{lat}}{Q_{sen}} = \frac{c_{pa} m_p (t_{p,in} - t_{p,out}) + h_{fg} m_p (\omega_{p,in} - \omega_{p,out})}{c_{pa} m_p (t_{p,in} - t_{p,out})} \quad (8)$$

With the η_{wb} and ε of an ERIEC system being predicted, the total heat recovery (Q_{tot}) can be calculated by Eq. (9). To evaluate the energy recovery achieved by ERIEC system, the $E_{recovery}$ shown in Eq. (10) is adopted by considering the overall coefficient of performance (COP) of the central cooling system that combining the ERIEC unit. In this study, the COP is set to be 4.5.

$$Q_{tot} = \varepsilon \eta_{wb} c_{pa} m_p (t_{p,in} - t_{wb,s}) \quad (9)$$

$$E_{recovery} = \frac{Q_{tot}}{COP} = \frac{\varepsilon \eta_{wb} c_{pa} m_p (t_{p,in} - t_{wb,s})}{COP} \quad (10)$$

For ERIEC operated under non-condensation conditions with only sensible heat transfer in the primary air, the ε equals to 1, and the cooling effectiveness can be estimated by the η_{wb} only. However, under condensation conditions, both η_{wb} and ε of the ERIEC system should be considered to assess the total heat recovery.

3. Derivation of simplified models

3.1 Modeling approach

It is noted from our previous studies [17], [31] that the variation trends of IEC cooling effectiveness with the inlet parameters show a twist after the condensation occurs in the primary air side. In this case, the simplified predicting models on ERIEC performance which suitable for hot and humid regions should be established in terms of condensation states and non-condensation states, respectively. The decision tree method can perform classification on the target variable based on predictor variables. By using the decision tree, whether the operating states of ERIEC should be 'non-condensation' or 'condensation' can be predicted. In the present study, the 2-level factorial designs were employed to determine whether certain factors or interactions between them have an effect on the cooling effectiveness of ERIEC system and to estimate the magnitude of that effect. According to literatures [16], [22], [28], the cooling effectiveness of ERIEC varies approximately linearly within the ranges of parameters under non-condensation or condensation states respectively, which makes the 2-level factorial design method suitable for the influence identification.

The flow chart of the statistical modeling approach for the practical predictive ERIEC model is shown in Fig. 3. Firstly, $1^{\#}$ simulation cases were generated by the numerical model at each selected parameter varying in certain ranges. Secondly, together with all available attributes working as training data set, the results of $1^{\#}$ simulations on the occurrence of condensation were used as binary target variables to build the decision tree for the classification on operation conditions. Next, with the decision rules extracted from the

decision tree-based model, the low and high values of selected parameters for different categories of operation condition can be defined, and the $2^{\#}$ simulations were carried out at all possible combinations of two levels of each factor considered. Last, based on the results of $2^{\#}$ simulations, the impact of each factor and their interactions on cooling effectiveness were examined quantitatively by a 2-level factorial design method. The linear regression equations on η_{wb} and ε of the ERIEC systems can be derived under the two categories (with and without condensation), respectively. Incorporating with the conditional expressions from the decision tree, the derived correlations can be used to predict the ERIEC performance under varying operation conditions taking into account the possible condensation of primary air.

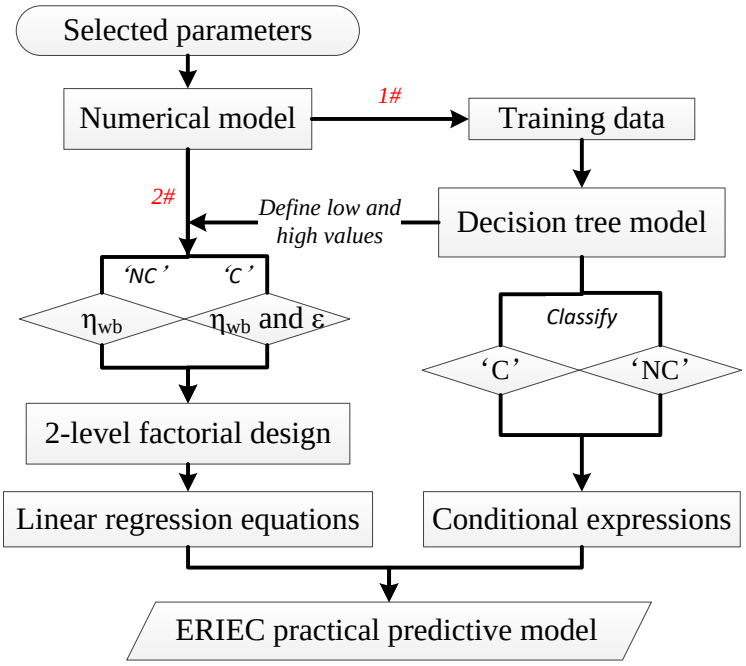

Fig. 3. Research flow chart of the practical predictive ERIEC model

Based on annual weather data and the design parameters of ERIEC system, the decision tree and decision rules can be utilized to classify the operation conditions into a 'condensation (C)' or 'non-condensation (NC)' category. The conditional functions concluded from decision rules and the developed correlations of ERIEC effectiveness can be easily incorporating with building simulation software. In this way, the annual energy recovery performance of the ERIEC system can be quickly estimated.

3.2 Identification of operation conditions (with/without condensation)

In terms of an ERIEC system operated in a specific building application, its cooling effectiveness is mainly influenced by the following factors: the inlet primary air temperature ($t_{p,in}$) and relative humidity ($RH_{p,in}$),

the inlet secondary air temperature ($t_{s,in}$) and relative humidity ($RH_{s,in}$), primary air flow volume (V_p), the ratio of primary to secondary air flow volume (m_{ratio}), the ratio of heat transfer area to primary air flow volume (A_{ratio}). These seven parameters, which are important determinants of the condensation in primary air, were selected as the input variables for the identification model adopting the decision tree method. The settings are given in Table 1 by considering the typical operation conditions for the ERIEC systems in hot and humid areas. With all the input variables evenly distributed in the range of values, a total of 4536 cases was simulated by the introduced numerical model of IEC in order to obtain the condensation ratio of each case.

Table 1. Input variables (or attributes) of the decision tree method

No.	Label	Unit	Value	Remark
1	$t_{p,in}$	℃	[28, 30, 32, 34, 36, 38, 40]	Typical climate conditions in hot and humid regions
2	$RH_{p,in}$	%	[40, 50, 60, 70, 80, 90]	
3	$t_{s,in}$	℃	[24, 26, 28]	Acceptable temperature and relative humidity ranges [48] of the indoor air (worked as secondary air)
4	$RH_{s,in}$	%	[40, 55, 70]	
5	m_{ratio}	-	[0.8, 1, 1.2]	Positive/negative air pressure requirement for the air-conditioned spaces
6	V_p	m^3/s	[0.5, 2]	A suitable range for air velocity considering pressure drop
7	A_{ratio}	$m^2/(m^3/s)$	[50, 250]	The NTU of the heat exchanger ranges from1 to 6

The decision tree method was employed to define the ranges of parameters for each ERIEC operation condition (with or without condensation), so as to provide the low and high values in the 2-level factorial designs. The target variable is expressed by the condensation ratio (R_{con}), defined as the proportion of the condensation area to the total heat exchanger area of coolers [45]. The state of $R_{con} = 0$ is considered as 'non-condensation', and state of $R_{con} > 0$ is considered as 'condensation'. C4.5 algorithm was used for training data set (three quarters of the cases which were arbitrarily selected) and test data set (the remained cases) by using WEKA to build a decision tree for predicting whether the operation of ERIEC should be classified as 'condensation (C)' or 'non-condensation (NC)'.

The decision tree is built on the basis of a training data set of 3402 cases with the 7 attributes listed in Table 1. It can be seen in Fig. 4 that this tree includes 11 nodes among which 6 are leaf nodes, represent there are 6 classes either 'NC' or 'C'. All the splitting tests in this decision tree are based on restrictions of inlet primary air temperature and relative humidity instead of other attributes, indicating that the occurrence of condensation in the ERIEC system is dominated by inlet primary air conditions. Each leaf node includes a

ratio showing how many percentages of cases fall into that class are in accordance with the corresponding classification result (‘NC’ or ‘C’), which can be regarded as the confidence level of the classification.

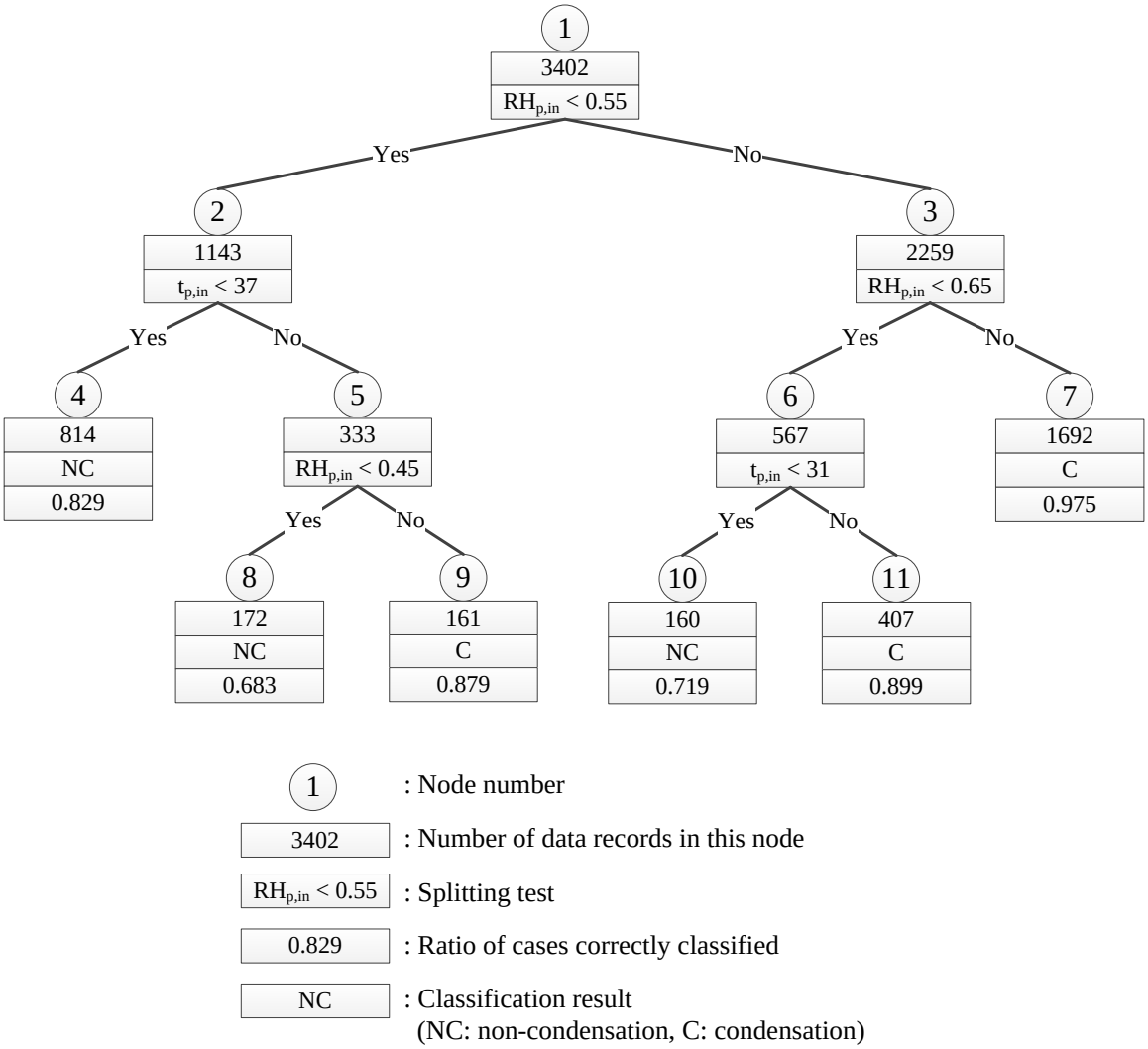

Fig. 4 Decision tree for the identification of ERIEC operation conditions

Based on a decision tree, the operation conditions with or without condensation can be easily identified through the conditional functions concluded from decision rules. Table 2 shows the complete set of decision rules which include all the executive routines from the root node to each leaf node.

Table 2 Decision rules derived from the decision tree

No.	Node	Decision rules
1	4	If $RH_{p,in} < 0.55$ and $t_{p,in} < 37$, then IEC is in ‘NC’ condition

2	7	If $RH_{p,in} \geq 0.65$, then IEC is in 'C' condition
3	8	If $RH_{p,in} < 0.45$ and $t_{p,in} \geq 37$, then IEC is in 'NC' condition
4	9	If $0.45 \leq RH_{p,in} < 0.55$ and $t_{p,in} \geq 37$, then IEC is in 'C' condition
5	10	If $0.65 \leq RH_{p,in} < 0.55$ and $t_{p,in} < 31$, then IEC is in 'NC' condition
6	11	If $0.65 \leq RH_{p,in} < 0.55$ and $t_{p,in} \geq 31$, then IEC is in 'C' condition

By calculating the proportion of simulation cases in condensation conditions, the probability of condensation under different inlet primary air states can be obtained. To clearly display the results derived from the decision tree model, eight zones were classified within the setting ranges of primary air temperature and relative humidity, as shown in Fig. 5. For Zone 1, the condensation is bound to happen even under the most unfavorable inlet secondary air conditions. By contrast, no condensation could occur if the inlet primary air state is in Zone 8. For other zones, the occurrence of condensation will depend on both the primary air inlet conditions and other input variables. However, even the other input variables vary within a range, the results of decision tree model showed that the identification of 'C' and 'NC' operation conditions is still dominated by inlet primary air states. It implies that the φ=55% can be drawn as a dividing line for the condensation achievable in the primary air with a temperature range of 31~37℃. For the primary air with temperature varies from 37℃ to 40℃, the dividing line on relative humidity goes down to 45%. For primary air temperature ranges from 28℃ to 31℃, the dividing line corresponds to a higher relative humidity (φ=65%). From the classification accuracy of the decision tree estimated by 1134 cases of the test data set, it indicates a good accuracy that 91% of all the training records can be correctly classified.

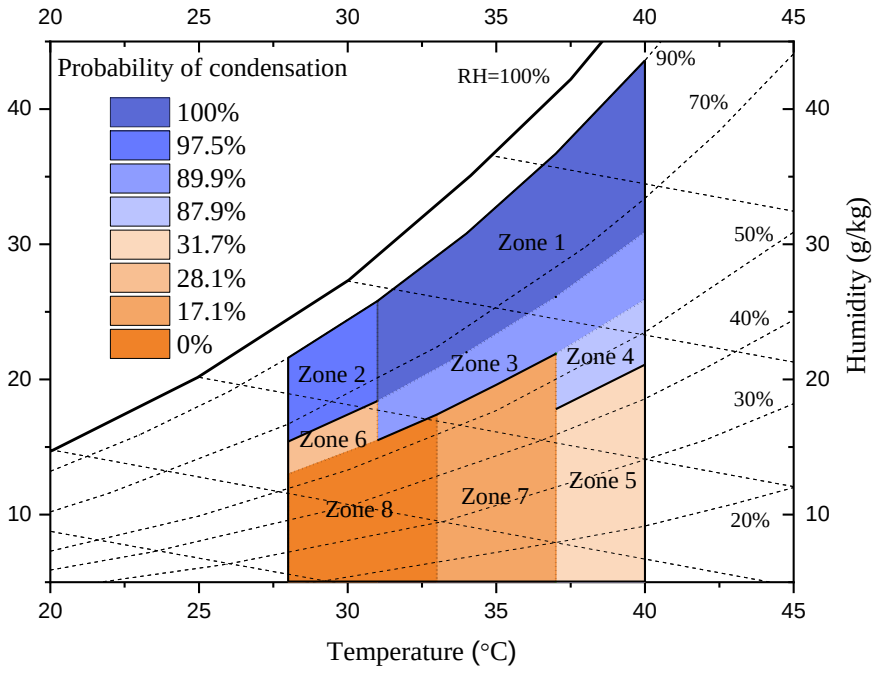

Fig. 5 Probability of condensation in different classification zones

3.3 Correlation development for ERIEC system

With the divided ranges extracted from the decision tree-based model, the 2-level factorial design can be carried out for non-condensation and condensation operation conditions of ERIEC system, respectively. Seven parameters listed in Table 3, which are important dominants for the IEC effectiveness, are selected to vary between a high value and a low value in the 2-level factorial design. The high and low levels of the selected parameters for the two different groups (non-condensation and condensation) were defined based on the classification of operation conditions presented in decision tree model and the typical application conditions for ERIEC systems in hot and humid areas.

Table 3. Factors and factor levels in the 2-level factorial design

No.	Parameter	Label	Unit	Non-condensation		Condensation	
				Low	High	Low	High
1	$t_{p,in}$	A	℃	28	33	33	40
2	$RH_{p,in}$	B	%	0.3	0.55	0.55	0.9
3	$t_{s,in}$	C	℃	24	28	24	28
4	$RH_{s,in}$	D	%	0.4	0.7	0.4	0.7
5	V_p	E	m^3/s	0.5	2	0.5	2
6	m_{ratio}	F	-	0.8	1.2	0.8	1.2
7	A_{ratio}	G	$m^2/(m^3/s)$	1	3	1	3

In order to derive the practical performance correlations of ERIEC system, simulations were carried out by the established numerical model with all possible combinations of each factor. Therefore, a set of 2^7=128 simulation cases were selected to correlate the indexes (η_{wb} and ε) for ERIEC system effectiveness under non-condensation conditions (Eq. (11)) and condensation conditions (Eq. (12-13)), respectively.

$$\eta_{wb,NC} = f(t_{p,in}, RH_{p,in}, t_{s,in}, RH_{s,in}, V_p, m_{ratio}, A_{ratio}) \quad (11)$$

$$\eta_{wb,C} = f(t_{p,in}, RH_{p,in}, t_{s,in}, RH_{s,in}, V_p, m_{ratio}, A_{ratio}) \quad (12)$$

$$\varepsilon = f(t_{p,in}, RH_{p,in}, t_{s,in}, RH_{s,in}, V_p, m_{ratio}, A_{ratio}) \quad (13)$$

3.3.1 Non-condensation conditions

For non-condensation condition with only sensible heat transfer in the ERIEC system, the 2-level factorial design was employed to analyze the effect of each influencing parameter and their interactions on the wet-

bulb efficiency ($\eta_{wb,NC}$). Three-factor interactions were involved in the model while upper product terms were ignored due to limited contribution. Based on simulation results, the effect of seven parameters and their interactions were examined quantitatively through a normal probability plot shown in Fig. 6. The effects of points fall on the fitted line as part of the normal distribution are considered insignificant. By contrast, points such as 'E' deviated at negative end and 'G' at positive end of the straight line have significant influences on the wet-bulb efficiency.

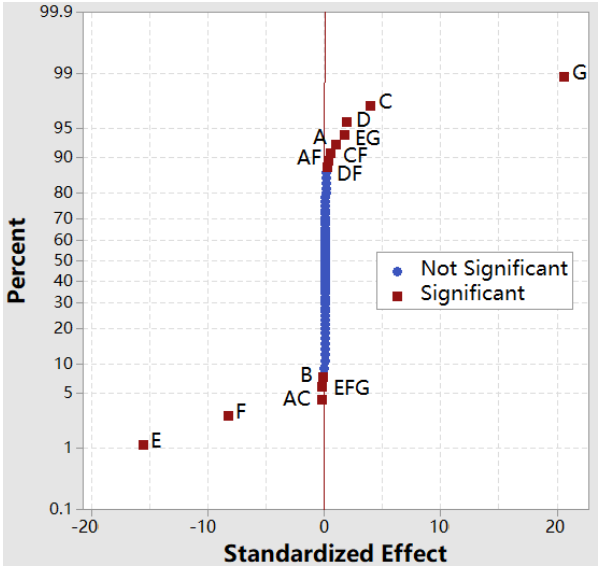

Fig. 6 Normal probability of standardized effects for non-condensation conditions

With the insignificant factors or interactions removed, the percentage contributions of the significant influence variables and interactions to the estimated variables were recomputed by the two-level design and shown in Table 4. Based on the regression coefficients, the linear regression model of the wet-bulb efficiency can be derived as a function (Eq. (14)) of selected parameters and interactions.

$$\begin{aligned}\eta_{wb,NC} = {} & \alpha_{const.} + \alpha_A t_{p,in} + \alpha_B RH_{p,in} + \alpha_C t_{s,in} + \alpha_D RH_{s,in} + \alpha_E V_p + \alpha_F m_{ratio} + \alpha_G A_{ratio} \\ & + \alpha_{AC} t_{p,in} t_{s,in} + \alpha_{AF} t_{p,in} m_{ratio} + \alpha_{CF} t_{s,in} m_{ratio} + \alpha_{DF} RH_{s,in} m_{ratio} \\ & + \alpha_{EG} V_p A_{ratio} + \alpha_{EFG} V_p m_{ratio} A_{ratio}\end{aligned} \tag{14}$$

Table 4 Percentage contributions and regression coefficients of the selected parameters for $\eta_{wb,NC}$

Parameter	A	B	C	D	E	F	G
Contribution (%)	1.73	0.29	7.16	3.33	28.77	15.30	37.77
Regression coefficient α_n	0.0031	-0.0087	0.0058	0.0141	-0.1375	-0.2608	0.0012

Parameter	AC	AF	CF	DF	EG	EFG
Contribution (%)	0.53	0.38	0.78	0.50	3.00	0.45
Regression coefficient α_n	-0.0001	0.0011	0.0023	0.0428	0.0004	-0.0002

* The subscript of α for each parameter is named by its corresponding label, e.g. $\alpha_A = 0.0031$.

* $\alpha_{const.} = 0.6820$.

3.3.2 Condensation conditions

Under the operating conditions with condensation, the ERIEC system provides both sensible cooling and dehumidification for the fresh air. In this way, both the wet-bulb effectiveness and enlargement coefficient should be considered to assess the total heat recovery performance. A 2-level factorial design was employed on the two indexes ($\eta_{wb,C}$ and ε) to correlate their equation models with the selected parameters. As shown in Fig. 7, normal probability plots are used for the identification of significant effects of the two performance indicators. Compared to the positive effect of factor 'A' ($t_{p,in}$) under non-condensation conditions (Fig. 4), in Fig. 5(a), the factor 'A' lies on the left side of the straight line and has a negative effect on the wet-bulb effectiveness under condensation conditions. The reason for the opposite effects is that the heat released through the condensation process raises the outlet primary air temperature as verified by other research [31, 46]. From Fig. 5(b), the factor 'B' ($RH_{p,in}$) has the largest effect on the enlargement coefficient because its point lies farthest from the line. The second important factor is 'A' ($t_{p,in}$) also on the right with positive effect.

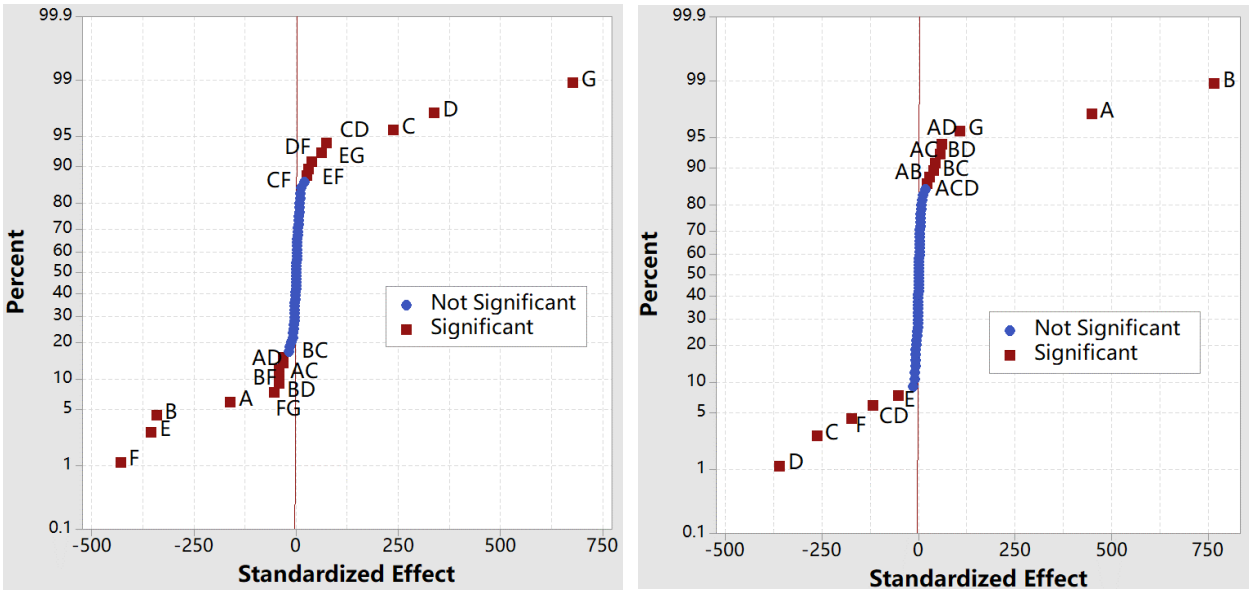

(a) wet-bulb efficiency ($\eta_{wb,C}$) (b) enlargement coefficient (ε)

Fig. 7 Normal probability of standardized effects for condensation conditions

The values of regression coefficients and estimated effects of the parameters on $\eta_{wb,C}$ and ε are presented in Table 5. The insignificant factors or interactions are negligible in the derived model. First-order linear regression equations for $\eta_{wb,C}$ and ε of the ERIEC system under condensation conditions are presented in Eq. (15) and (16).

$$\begin{aligned}\eta_{wb,C} = {} & \alpha'_{const.} + \alpha'_A t_{p,in} + \alpha'_B RH_{p,in} + \alpha'_C t_{s,in} + \alpha'_D RH_{s,in} + \alpha'_E V_p + \alpha'_F m_{ratio} + \alpha'_G A_{ratio} \\ & + \alpha'_{AC} t_{p,in} t_{s,in} + \alpha'_{AD} t_{p,in} RH_{s,in} + \alpha'_{BC} RH_{p,in} t_{s,in} + \alpha'_{BD} RH_{p,in} RH_{s,in} \\ & + \alpha'_{BF} RH_{p,in} m_{ratio} + \alpha'_{CD} RH_{s,in} + \alpha'_{CF} t_{s,in} m_{ratio}\end{aligned} \quad (15)$$

$$\begin{aligned}\varepsilon = {} & \beta_{const.} + \beta_A t_{p,in} + \beta_B RH_{p,in} + \beta_C t_{s,in} + \beta_D RH_{s,in} + \beta_E V_p + \beta_F m_{ratio} + \beta_G A_{ratio} \\ & + \beta_{AB} t_{p,in} RH_{p,in} + \beta_{AC} t_{p,in} t_{s,in} + \beta_{AD} t_{p,in} RH_{s,in} + \beta_{BC} RH_{p,in} t_{s,in} + \beta_{CD} t_{s,in} RH_{s,in} \\ & + \beta_{ACD} t_{p,in} t_{s,in} RH_{s,in}\end{aligned} \quad (16)$$

Table 5 Percentage contributions and regression coefficients of the selected parameters for $\eta_{wb,C}$ and ε

$\eta_{wb,C}$	Parameter	A	B	C	D	E	F	G
	Contribution (%)	5.37	11.38	7.85	11.20	11.80	14.29	22.46
	Regression coefficient α'_n	0.0230	0.7290	0.0439	0.4399	-0.1072	-0.1021	0.0009
	Parameter	AC	AD	BC	BD	BF	CD	CF
	Contribution (%)	1.07	1.39	1.06	1.40	1.40	2.41	0.86
	Regression coefficient α'_n	-0.0009	-0.0156	-0.0266	-0.4706	-0.3520	0.0202	0.0054
	Parameter	DF	EF	EG	FG			
	Contribution (%)	1.24	0.94	2.05	1.82			
	Regression coefficient α'_n	0.1044	0.0237	0.0001	-0.0003			
ε	Parameter	A	B	C	D	E	F	G
	Contribution (%)	17.63	30.18	10.41	14.24	2.13	6.90	4.18
	Regression coefficient β_n	0.0772	-5.4510	0.0852	16.400	-0.0514	-0.4154	0.0006
	Parameter	AB	AC	AD	BC	BD	CD	ACD
	Contribution (%)	1.07	1.71	2.38	1.50	2.19	4.67	0.80
	Regression coefficient β_n	0.1712	-0.0048	-0.4260	0.1811	3.5190	-0.9440	0.0213

* The subscript of α′ and β for each parameter is named by its corresponding label, e.g. $\alpha'_A = 0.0230$.

* $\alpha'_{const.} = -0.4400$. $\beta_{const.} = -0.8600$.

4. Model validation

The accuracy of the practical predictive model was validated by using both lab experimental data and field-measurement data. Firstly, the lab experimental data from literature were used to validate the model-predicted effectiveness under non-condensation and condensation conditions, respectively. Then, the field-measurement data was collected in Hong Kong and compared with the model-predicted sensible and latent heat transfer effectiveness. In this way, the reliability of the proposed practical model in predicting the performance of ERIEC systems in real buildings can be validated.

4.1 Experimental validation

The validation of the effectiveness correlations in this practical predictive model was conducted by comparing with the experimental results in the previous study [46]. This published paper investigated the performance of a plate-type cross-flow IEC under the low/high air humidity operating mode. Under high humidity inlet air, the condensation took place and the latent efficiency of the cooler was calculated by the measured inlet and outlet air humidity. The geometric parameters of the experimental heat exchanger module are shown in Table 6. By setting the same inlet parameters with the experimental conditions, the model-predicted effectiveness values can be validated under both the operation states with or without condensation.

Table 6 Geometric parameters of the experimental heat exchanger module

Parameter	Units	Value
Number of air channels (n)	-	50
Channel gap (s)	mm	4
Channel length (L)	m	0.4
Channel height (H)	m	0.4
Heat transfer area (A)	m^2	8

Due to the measuring errors during the tests, the uncertainty associated with the measured ERIEC's effectiveness should be determined to provide more reasonable data for the validation. As shown in Table 7, the uncertainties of the experimental results were examined under low and high humidity of inlet primary air for non-condensation and condensation states respectively. The uncertainty analysis of the measuring data and calculated performance indicators are determined using the method in reference [47].

Table 7 Uncertainty analysis of the experimental results

Parameter	Nominal value	Uncertainty

	Low humidity	High humidity	Low humidity	High humidity
u_p	2.0 m/s	2.0 m/s	±4.5%	±4.5%
u_s	2.5 m/s	2.5 m/s	±3.6%	±3.6%
t_p	30 ℃	30 ℃	±0.6%	±0.6%
RH_p	45%	75%	±2.1%	±1.2%
η_{wb}	0.61	0.51	±4.2%	±4.8%
ε	1	2.31	-	±12.7%

* Low humidity: u_p = 2.0 m/s, u_s = 2.5 m/s, t_p = 30℃, RH_p = 45%, t_p = 22.5℃, RH_s = 68%.

* High humidity: u_p = 2.0 m/s, u_s = 2.5 m/s, t_p = 30℃, RH_p = 75%, t_p = 22.5 ℃, RH_s = 68%.

4.1.1 Non-condensation conditions

Under experimental conditions, it is difficult to keep the other inlet parameters stable when changing the value of one inlet parameter. For the tested non-condensation operation states, the inlet primary air relative humidity varies between 37.4% to 58.9%. The experimental results of η_{wb} for non-condensation conditions exhibit the uncertainty of 4.2%. Fig. 8 (a) and (b) present the measured and model-predicted wet-bulb efficiency under different inlet primary air temperature and velocity. It can be seen that the two sets of data are well coincident with the discrepancy lower than 9.52% under different inlet primary air temperature and 4.27% under different inlet primary air velocity.

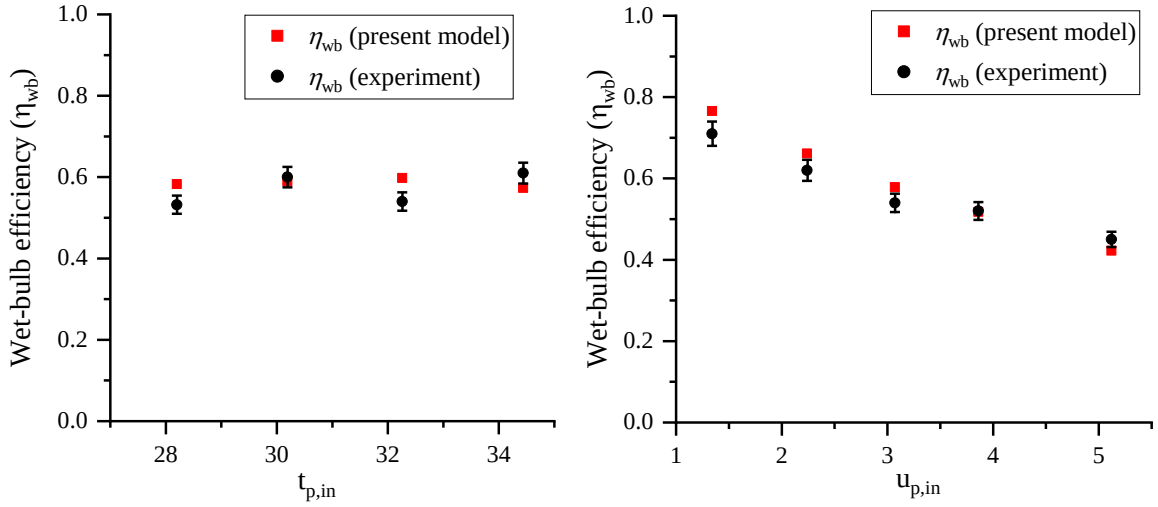

(a) different primary air temperature (b) different primary air velocity

Fig. 8 Comparison between experimental and model-predicted effectiveness values under non-condensation conditions

4.1.2 Condensation conditions

Under the simulation cases with condensation, the inlet primary air relative humidity varies between 57.1% to 86.4%. The relative humidity of the outlet primary air is nearly 100%. The performance indicators of η_{wb} and ε were predicted by the practical model under the same inputs as measured in the test. The experimental results of η_{wb} and ε for condensation conditions exhibit the uncertainty of 4.8% and 12.7%, respectively. The comparison between the measured and model-predicted wet-bulb efficiency under different inlet primary air temperature and velocity are shown in Fig. 9 (a) and (b). It was found that a discrepancy within 8.16% can be realized in predicting the η_{wb} for condensation states. The discrepancy between predicted and measured values of ε is 7.69%, which is within the uncertainty range of the measured results.

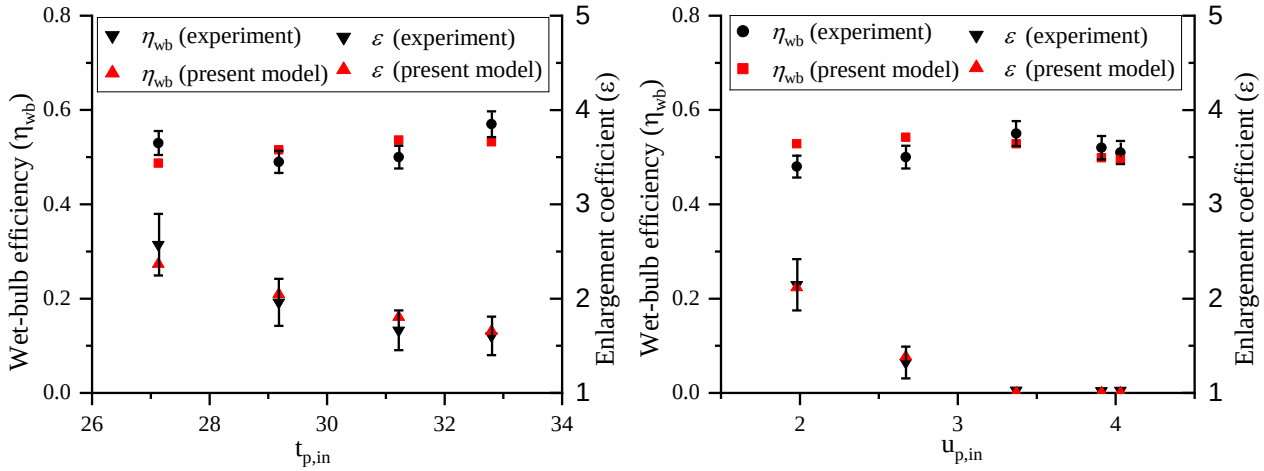

(a) different primary air temperature (b) different primary air velocity

Fig. 9 Comparison between experimental and model-predicted effectiveness values under condensation conditions

From the experimental validation, the model-predicted values agreed well with the measured values, within the discrepancy of 10% in η_{wb} and ε. The 10% deviation threshold indicates that the differences between measured and predicted values are lower than 1°C [35] on produced air temperature and 15% on total heat transfer rate, which is acceptable for the proposed predictive model to be used in the energy performance assessment of ERIEC system.

4.2 Field-measurement validation

4.2.1 Test overview

In order to estimate the accuracy of the proposed model for the ERIEC operated under varying outdoor climates, a field measurement has been conducted in a wet market located in Tung Chung area, Hong Kong. The wet market is a one-story building with a floor area of 260m^2 and a height of 6.7m. The central air-conditioning system in this wet market operates under all fresh air mode. This prototype of ERIEC was produced by a cooperated manufacturer based on the design parameters listed in Table 8. Fig. 10 shows the air ducts arrangement of the packed ERIEC system, which consists of an air-to-air plate heat exchanger, primary and secondary air fans, a water pump and water spraying devices.

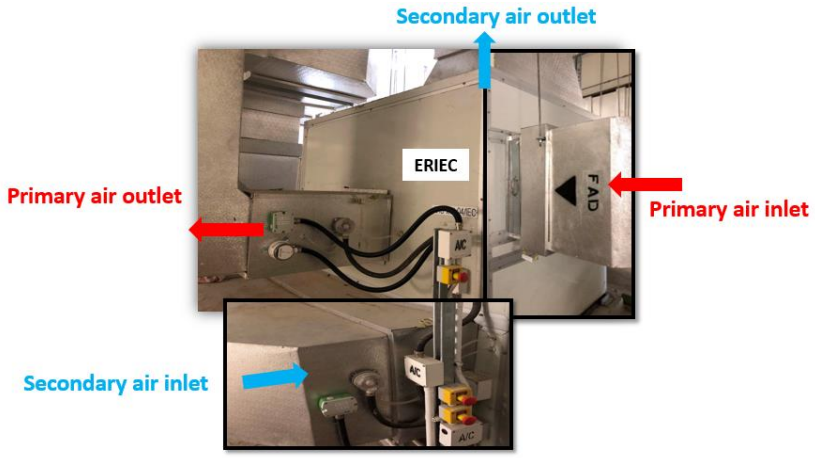

Fig.10 Air ducts arrangement of the packed ERIEC system in a wet market

Table 8 Configurations of the ERIEC system in the wet market

Parameter	Units	Value
Primary air flow volume (V_p)	m^3/h	5400
Secondary air flow volume (V_s)	m^3/h	6000
Ratio of primary to secondary air flow volume (m_{ratio})	-	0.9
Number of air channels (n)	-	200
Channel gap (s)	mm	4
Channel length (L)	m	1
Channel height (H)	m	1
Heat transfer area (A)	m^2	200

The energy recovery performance of this trial ERIEC system was tested under the constant air flow volume operation mode for dynamic cooling load in the wet market. The test duration lasted for 30 days in a cooling season. The system operates for 14 hours per day, from 6:30~20:30. Fig. 11 shows the schematic of the sensor settings for the ERIEC system. For the traditional IEC which sensibly cools the fresh air, only the temperature data on inlet and outlet air need to be collected. However, for the ERIEC operated in humid regions, the moisture content of fresh air should also be measured to fully take into account the total heat recovery in the situation that condensation occurs. In this system, a data logger was used to monitor and collect the measured parameters from the sensors including air temperature, relative humidity and velocity. Table 9 indicates all the measured parameters and specifications of measuring instruments. The setting on the time interval for measurement is 1 minute.

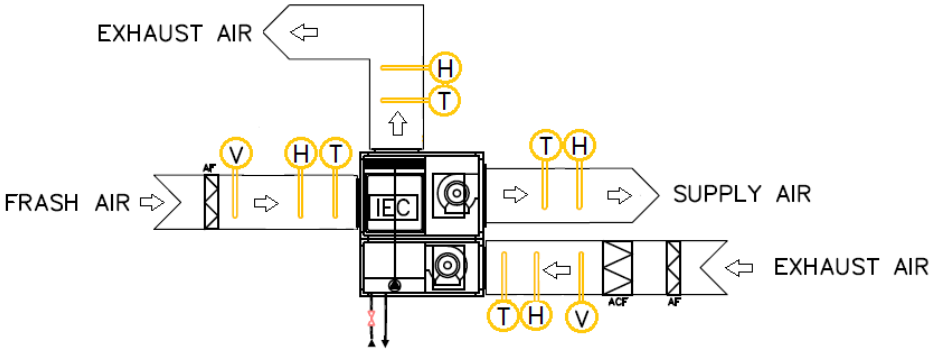

Fig. 11 Schematic diagram of the sensor settings

Table 9. The measured parameters and the specification of the measuring instruments

Parameter	Instrument	Range	Accuracy
Temperature	EE160	-15~60℃	±0.3℃
Humidity	EE160	10~95% RH	±2.5% RH
Air velocity	EE65	0~10 m/s	±0.2m/s

4.2.2 Result analysis

Two typical days of the test period were selected to compare the predicted and measured values on the performance of ERIEC system. Fig. 12 shows the inlet and outlet temperature and humidity of the primary air for two days, and the gray areas represent the operation duration of the ERIEC system. It is noted that the ERIEC system consistently delivered 21°C ~ 25°C fresh air with the outdoor temperature fluctuated between 26°C to 33°C. During most of the operation time in the first day, the moisture content of primary air on the outlet was lower than that on the inlet, indicating that the fresh air was not only cooled but also

dehumidified. In the second day, with the outdoor air relative humidity decreased from 80% at 6:30 to 50% at 14:40, the condensation of primary air occurred at first and then the moisture content of primary air on the inlet and outlet maintained at similar levels.

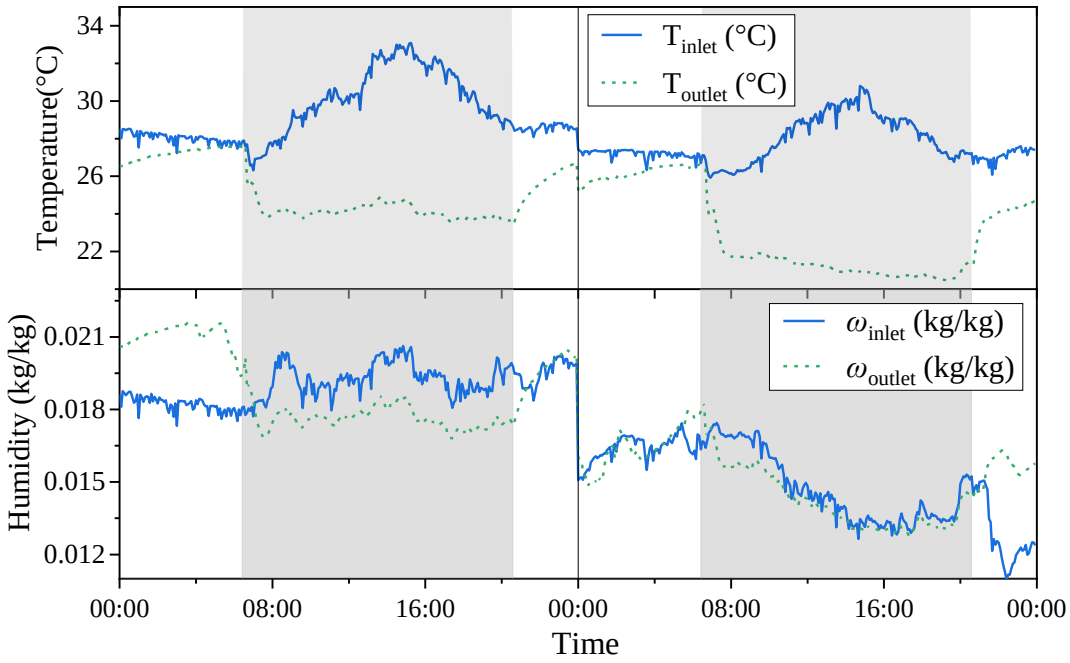

Fig. 12 Temperature and humidity variation of primary air

When the ERIEC system is operated in a real building, the condensation of fresh air is dependent on the varying ambient weather conditions. The proposed simplified predicting model could rapidly determine if the operation condition leads to condensation, and assign the corresponding performance correlations for non-condensation or condensation conditions respectively. Fig. 13 shows a comparison of model-predicted effectiveness values and the actual operating performance of the ERIEC system from field-measurement results. It can be seen that the model-predicted values on wet-bulb efficiency and enlargement coefficient agree well with the measured values under both non-condensation and condensation conditions. The measured effectiveness values fluctuate widely during the first 1 hour after starting the system because of the unsteady states. The discrepancy on wet-bulb efficiency and enlargement coefficient are within 7.1% and 5.7% during 95% percentage of the operation time in these two days.

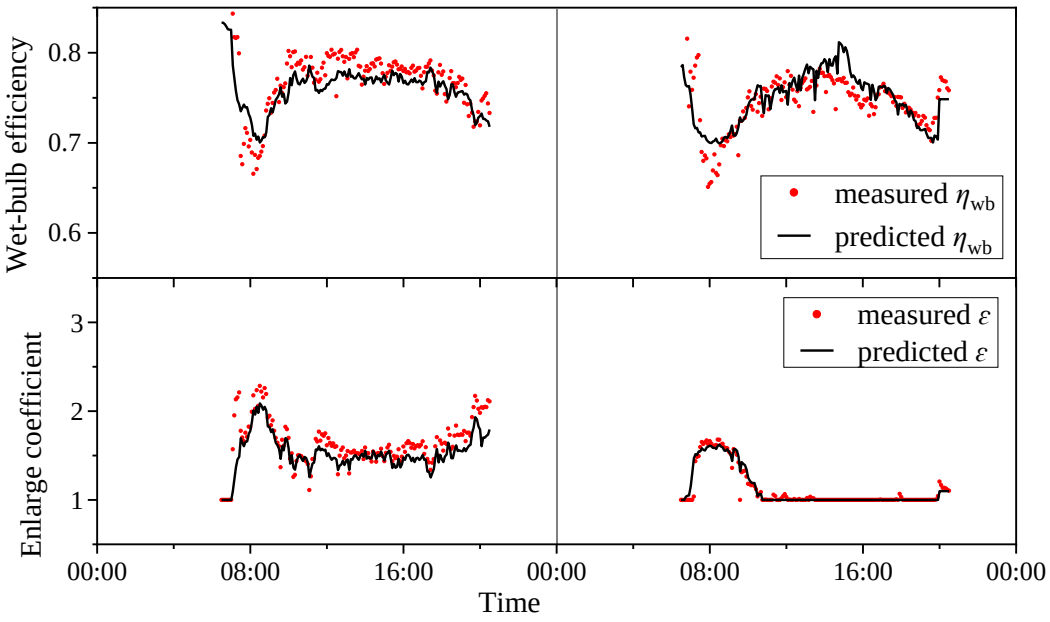

Fig. 13 Comparison between measured and model-predicted effectiveness values (η_{wb} and ε)

With the predicted or measured performance indexes (η_{wb} and ε), the total heat recovery achieved by the ERIEC system can be obtained. Fig. 14 shows the comparison between predicted and measured results of the total heat recovery (Q_{tot}) during the test duration. During the test period, the outdoor air temperature ranges from 24°C to 35°C, and the relative humidity ranges from 40% to 95%. As the ERIEC system runs 14 hours per day with the test interval of 1minite, the simplification was processed to average the 60 values from each hour and to plot these as a complete sequence. It can be seen from Fig. 10 that the model-predicted values fit the measured results well with the same variation trends. Due to the unsteady operation conditions of the ERIEC system which affect the heat and mass transfer process, the measured total heat recovery performance is lower than that of predicted value during most of the test period. The largest discrepancy between predicted and measured results on total heat recovery is 19.2%.

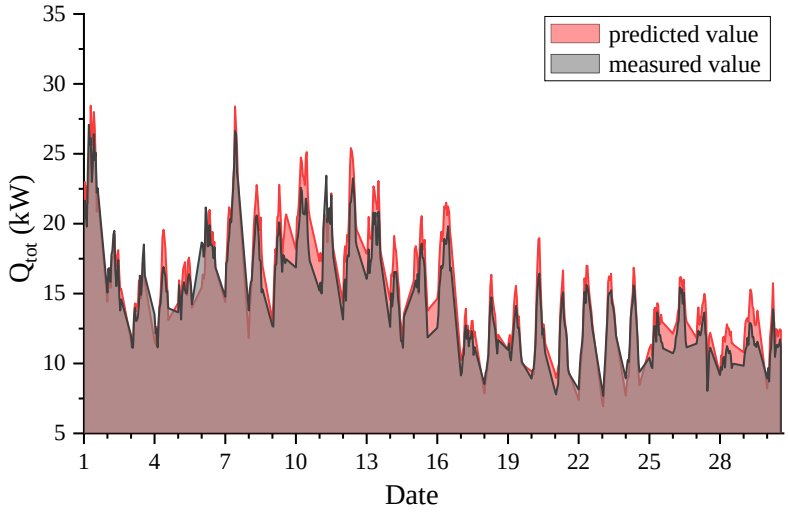

Fig. 14 Comparison between measured and model-predicted results in total heat recovery

By accumulating the hourly amount of energy recovery achieved by the ERIEC system during the test periods, the total energy recovery ($E_{recovery}$) for the cooling season can be obtained. The predicted and measured results of $E_{recovery}$ for per unit floor area are 5.85 kWh/m^2 and 5.40 kWh/m^2 respectively during the test duration of 30 days, with a discrepancy of 8.4%. Moreover, two standardized statistical indices were adopted to assess the calibration of the proposed simplified models, including the mean bias error (MBE) and coefficient of variation of root mean square error (CVRMSE) [48]. The validation of the predicting model was conducted based on the average values for each hour from measurement and simulation. The hourly sensible heat recovery, latent heat recovery and energy recovery achieved by the ERIEC system during the test period were calibrated with the standardized statistical indices shown in Table 10. From the calibration results, the MBE for all the predicted parameters is less than 10%, with the CVRMSE no larger than 30%. As it meets the hourly criteria set out by ASHRAE Guideline 14 [49], the proposed predicting model can be considered as validated.

Table 10. Calibration of the predicting model on the performance of ERIEC system

Parameter	Standardized statistical indices (%)	
	MBE	CVRMSE
Sensible heat recovery (Q_{sen})	9.1	13.2
Latent heat recovery (Q_{lat})	3.5	29.5
Energy recovery ($E_{recovery}$)	8.5	13.3

5. Conclusions

In this study, a statistical modeling approach was proposed for the performance prediction of indirect evaporative cooling energy recovery system (ERIEC). Combining the decision tree model and 2-level factorial design method, the developed model can be of practical use to predict both the sensible cooling and dehumidifying performance of the ERIEC in hot and humid regions. Model validation was conducted by comparing the predicted and experimental data of an ERIEC under various operating conditions with or without condensation. Besides, the field measurement was carried out on a trail ERIEC system in Hong Kong to validate the practical predictive model under varying outdoor climates. The proposed practical model could benefit the promotion of ERIEC applications in hot and humid regions by providing efficient performance prediction for building energy assessment. The main results are as follows.

- Based on the training data extracted from a validated numerical model of plate-type indirect evaporative coolers, a decision tree model was established to identify the operation conditions (with or without condensation) of the ERIEC. The derived conditional expressions were used to judge the occurrence of condensation from primary air in the ERIEC according to inlet air temperature and relative humidity. It is indicated that the condensation will occur when the outdoor relative humidity is higher than 55% with a temperature range of 31~37℃.
- Using the 2-level factorial design, the major parameters and interactions significantly affect the performance of the ERIEC can be determined. It showed that the increase of inlet primary air temperature can improve the wet-bulb efficiency (η_{wb}) under non-condensation states and decrease the η_{wb} under condensation states. First-order linear regressions on the indicators of sensible cooling and dehumidification performance were correlated respectively.
- The experimental validation shows that the model-predicted results of ERIEC agree well with the experimental data. The discrepancy in predicting the η_{wb} is within 9.5% for non-condensation states and 4.3% for condensation states. The deviations between predicted and measured values of the enlargement coefficient (ε) are within the uncertainty ranges of the measured results.
- Comparing to the tested results of the trail ERIEC system under varying outdoor climates, this model can achieve the prediction accuracy within ±7.1% on η_{wb} and ±5.7% on ε during 95% percentage of the operation time. During a test duration of 30 days in the cooling season, the measured and predicted total energy recovery of ERIEC are 5.85 kWh/m^2 and 5.40 kWh/m^2 respectively, with a discrepancy of 8.4%.

Acknowledgment

The authors wish to acknowledge the financial support provided by the Research Institute of Sustainable Urban Development of The Hong Kong Polytechnic University and the field test collaboration from the Housing

Authority of the Hong Kong SAR Government.

References:

[1] She X, Cong L, Nie B, Leng G, Peng H, Chen Y, et al. Energy-efficient and -economic technologies for air conditioning with vapor compression refrigeration: A comprehensive review. Applied Energy. 2018;232:157-86.
[2] Hasan A. Going below the wet-bulb temperature by indirect evaporative cooling: Analysis using a modified ε-NTU method. Applied Energy. 2012;89:237-45.
[3] Rampazzo M, Lionello M, Beghi A, Sisti E, Cecchinato L. A static moving boundary modelling approach for simulation of indirect evaporative free cooling systems. Applied Energy. 2019;250:1719-28.
[4] Zheng B, Guo C, Chen T, Shi Q, Lv J, You Y. Development of an experimental validated model of cross-flow indirect evaporative cooler with condensation. Applied Energy. 2019;252:113438.
[5] Velasco Gómez E, Tejero González A, Rey Martínez FJ. Experimental characterisation of an indirect evaporative cooling prototype in two operating modes. Applied Energy. 2012;97:340-6.[6] Riangvilaikul B, Kumar S. An experimental study of a novel dew point evaporative cooling system. Energy and Buildings. 2010;42:637-44.
[7] Oh SJ, Shahzad MW, Burhan M, Chun W, Kian Jon C, KumJa M, et al. Approaches to energy efficiency in air conditioning: A comparative study on purge configurations for indirect evaporative cooling. Energy. 2019;168:505-15.
[8] Bajwa M, Aksugur E, Al-Otaibi G. The potential of the evaporative cooling techniques in the gulf region of the Kingdom of Saudi Arabia. Renewable Energy. 1993;3:15-29.
[9] Maheshwari G, Al-Ragom F, Suri R. Energy-saving potential of an indirect evaporative cooler. Applied Energy. 2001;69:69-76.
[10] Delfani S, Esmaeelian J, Pasdarshahri H, Karami M. Energy saving potential of an indirect evaporative cooler as a pre-cooling unit for mechanical cooling systems in Iran. Energy and Buildings. 2010;42:2169-76.
[11] Wan Y, Lin J, Chua KJ, Ren C. Similarity analysis and comparative study on the performance of counter-flow dew point evaporative coolers with experimental validation. Energy Conversion and Management. 2018;169:97-110.
[12] Cianfrini C, Corcione M, Habib E, Quintino A. Energy performance of air-conditioning systems using an indirect evaporative cooling combined with a cooling/reheating treatment. Energy and Buildings. 2014;69:490-7.
[13] Chen Y, Yan H, Yang H. Comparative study of on-off control and novel high-low control of regenerative indirect evaporative cooler (RIEC). Applied Energy. 2018;225:233-43.
[14] Cui X, Chua K, Yang W. Use of indirect evaporative cooling as pre-cooling unit in humid tropical climate: an energy saving technique. Energy Procedia. 2014;61:176-9.
[15] De Antonellis S, Joppolo CM, Liberati P, Milani S, Romano F. Modeling and experimental study of an indirect evaporative cooler. Energy and Buildings. 2017;142:147-57.
[16] Heidarinejad G, Moshari S. Novel modeling of an indirect evaporative cooling system with cross-flow configuration. Energy and Buildings. 2015;92:351-62.
[17] Min Y, Chen Y, Yang H. Numerical study on indirect evaporative coolers considering condensation: A thorough comparison between cross flow and counter flow. International Journal of Heat and Mass Transfer. 2019;131:472-86.
[18] Zhou Y, Zhang T, Wang F, Yu Y. Performance analysis of a novel thermoelectric assisted indirect evaporative cooling system. Energy. 2018;162:299-308.

[19] Wen T, Lu L, Zhong H, Dong C. Experimental and numerical study on the regeneration performance of LiCl solution with surfactant and nanoparticles. International Journal of Heat and Mass Transfer. 2018;127:154-64.
[20] Zhan C, Duan Z, Zhao X, Smith S, Jin H, Riffat S. Comparative study of the performance of the M-cycle counter-flow and cross-flow heat exchangers for indirect evaporative cooling – Paving the path toward sustainable cooling of buildings. Energy. 2011;36:6790-805.
[21] Woods J, Kozubal E. A desiccant-enhanced evaporative air conditioner: Numerical model and experiments. Energy Conversion and Management. 2013;65:208-20.
[22] Riangvilaikul B, Kumar S. Numerical study of a novel dew point evaporative cooling system. Energy and Buildings. 2010;42:2241-50.
[23] Lin J, Wang RZ, Kumja M, Bui TD, Chua KJ. Multivariate scaling and dimensional analysis of the counter-flow dew point evaporative cooler. Energy Conversion and Management. 2017;150:172-87.
[24] Pakari A, Ghani S. Comparison of 1D and 3D heat and mass transfer models of a counter flow dew point evaporative cooling system: Numerical and experimental study. International Journal of Refrigeration. 2019;99:114-25.
[25] Pandelidis D, Anisimov S. Numerical analysis of the heat and mass transfer processes in selected M-Cycle heat exchangers for the dew point evaporative cooling. Energy Conversion and Management. 2015;90:62-83.
[26] Chen Y, Yang H, Luo Y. Investigation on solar assisted liquid desiccant dehumidifier and evaporative cooling system for fresh air treatment. Energy. 2018;143:114-27.
[27] Wan Y, Ren C, Xing L. An approach to the analysis of heat and mass transfer characteristics in indirect evaporative cooling with counter flow configurations. International Journal of Heat and Mass Transfer. 2017;108:1750-63.
[28] Cui X, Chua KJ, Yang WM. Numerical simulation of a novel energy-efficient dew-point evaporative air cooler. Applied Energy. 2014;136:979-88.
[29] REN C-q, ZHANG L-a. Used CFD for the three-dimensions numerical simulation of the indirect evaporative cooler [J]. Energy Conservation. 2005;6:003.
[30] Wen T, Luo Y, He W, Gang W, Sheng L. Development of a novel quasi-3D model to investigate the performance of a falling film dehumidifier with CFD technology. International Journal of Heat and Mass Transfer. 2019;132:431-42.
[31] Chen Y, Yang H, Luo Y. Indirect evaporative cooler considering condensation from primary air: Model development and parameter analysis. Building and Environment. 2016;95:330-45.
[32] Chen Y, Yang H, Luo Y. Parameter sensitivity analysis and configuration optimization of indirect evaporative cooler (IEC) considering condensation. Applied Energy. 2017;194:440-53.
[33] Meng D, Lv J, Chen Y, Li H, Ma X. Visualized experimental investigation on cross-flow indirect evaporative cooler with condensation. Applied Thermal Engineering. 2018;145:165-73.
[34] Pandelidis D, Cichoń A, Pacak A, Anisimov S, Drąg P. Performance comparison between counter- and cross-flow indirect evaporative coolers for heat recovery in air conditioning systems in the presence of condensation in the product air channels. International Journal of Heat and Mass Transfer. 2019;130:757-77.
[35] Kim M-H, Jeong D-S, Jeong J-W. Practical thermal performance correlations for a wet-coil indirect evaporative cooler. Energy and Buildings. 2015;96:285-98.
[46] Cui X, Islam MR, Mohan B, Chua KJ. Developing a performance correlation for counter-flow regenerative indirect evaporative heat exchangers with experimental validation. Applied Thermal Engineering. 2016;108:774-84.
[37] Pandelidis D, Anisimov S. Application of a statistical design for analyzing basic performance characteristics of the cross-flow Maisotsenko cycle heat exchanger. International Journal of Heat and Mass Transfer. 2016;95:45-61.

[38] Wen T, Lu L. A review of correlations and enhancement approaches for heat and mass transfer in liquid desiccant dehumidification system. Applied Energy. 2019;239:757-84.
[39] Sohani A, Sayyaadi H, Hasani Balyani H, Hoseinpoori S. A novel approach using predictive models for performance analysis of desiccant enhanced evaporative cooling systems. Applied Thermal Engineering. 2016;107:227-52.
[40] Jafarian H, Sayyaadi H, Torabi F. Modeling and optimization of dew-point evaporative coolers based on a developed GMDH-type neural network. Energy Conversion and Management. 2017;143:49-65.
[41] Sohani A, Sayyaadi H, Hoseinpoori S. Modeling and multi-objective optimization of an M-cycle cross-flow indirect evaporative cooler using the GMDH type neural network. International Journal of Refrigeration. 2016;69:186-204.
[42] Sohani A, Sayyaadi H, Mohammadhosseini N. Comparative study of the conventional types of heat and mass exchangers to achieve the best design of dew point evaporative coolers at diverse climatic conditions. Energy Conversion and Management. 2018;158:327-45.
[43] Chengqin R, Hongxing Y. An analytical model for the heat and mass transfer processes in indirect evaporative cooling with parallel/counter flow configurations. International Journal of Heat and Mass Transfer. 2006;49:617-27.
[44] ASHRAE A, Standard A. 55, 2013. Thermal Environmental Conditions for Human Occupancy, American Society Of Heating, Ventilating and Air-conditioning Engineers, Atlanta.
[45] Chen Y, Luo Y, Yang H. A simplified analytical model for indirect evaporative cooling considering condensation from fresh air: Development and application. Energy and Buildings. 2015;108:387-400.
[46] Chen Y, Yang H, Luo Y. Experimental study of plate type air cooler performances under four operating modes. Building and Environment. 2016;104:296-310.
[47] Coleman HW, Steele WG. Experimentation, validation, and uncertainty analysis for engineers: John Wiley & Sons; 2018.
[48] Coakley D, Raftery P, Keane M. A review of methods to match building energy simulation models to measured data. Renewable and sustainable energy reviews. 2014;37:123-41.
[49] Guideline A. Guideline 14-2002. Measurement of energy and demand savings. 2002;22.